Concurrent measurements of soil and ecosystem respiration in a mature eucalypt woodland: advantages, lessons, and questions

Authors: A. A. Renchon[1, 6], J. E. Drake[2], C.A. Macdonald[1], D. Sihi[3], N. Hinko-Najera[4], M. G. Tjoelker[1], S. K. Arndt[4], N. J. Noh[1], E. Davidson[5], E. Pendall[1]

[1]Hawkesbury Institute for the Environment, Western Sydney University, Penrith, NSW, Australia

[2]SUNY College of Environmental Science and Forestry, Syracuse, New York, USA

[3]Department of Environmental Sciences, Emory University, Atlanta, Georgia, USA

[4]School of Ecosystem and Forest Sciences, The University of Melbourne, Richmond, 3121, Victoria, Australia

[5]University of Maryland Center for Environmental Science Appalachian Laboratory, Frostburg, Maryland, USA

[6]New address: Argonne National Laboratory, Environmental Science Division (EVS), Lemont, Illinois, USA

This is the author manuscript accepted for publication and has undergone full peer review but has not been through the copyediting, typesetting, pagination and proofreading process, which may lead to differences between this version and the Version of Record. Please cite this article as doi: 10.1029/2020JG006221.

Abstract

Understanding seasonal and diurnal dynamics of ecosystem respiration (R_{eco}) in forests is challenging, because R_{eco} can only be measured directly during night-time by eddy-covariance flux towers. R_{eco} is the sum of soil respiration (R_{soil}) and above-ground respiration (in theory, $R_{AG} = R_{eco} - R_{soil}$). R_{soil} can be measured day and night and can provide a check of consistency on R_{eco}, as the difference in magnitude and time dynamic between R_{eco} and R_{soil} should be explained by R_{AG}. We assessed the temporal patterns and climatic drivers of R_{soil} and R_{eco} in a mature eucalypt woodland, using continuous measurements (only at night for R_{eco}) at half-hourly resolution over 4 years (2014-2017). Our data showed large seasonal and diurnal (overnight) variation of R_{eco}, while R_{soil} had a low diurnal amplitude and their difference ($R_{eco} - R_{soil,}$ or R_{AG}) had a low seasonal amplitude. This result implies at first glance that seasonal variation of R_{eco} was mainly influenced by R_{soil} while its diurnal variation was mainly influenced by R_{AG}. However, our analysis suggests that the night-time R_{eco} decline cannot realistically be explained by a decline of R_{AG}. Chamber measurements of autotrophic components at half-hourly time resolution are needed to quantify how much of the R_{eco} decline overnight is due to declines in leaf or stem respiration, and how much is due to missing storage or advection, which may create a systematic bias in R_{eco} measurements. Our findings emphasize the need for reconciling bottom-up (via components measured with chambers) and direct estimates of R_{eco} (via eddy-covariance method).

- Seasonal and diurnal dynamics of soil respiration were used to constrain ecosystem respiration over four years
- Overnight decline in ecosystem respiration could not be explained by soil or aboveground respiration, suggesting measurement bias
- Measurements of fluxes and temperature sensitivity of autotrophic respiration components are needed to reduce ecosystem scale uncertainties

Plain Language Summary

Climate is changing rapidly, mostly because of increasing atmospheric CO_2 resulting from human-caused emissions. An important question regarding climate change mitigation is: will land continue to absorb human-caused CO_2 emissions? To address this question, the net exchange of CO_2 between ecosystem and the atmosphere has been measured globally by a network of flux towers. Flux towers rely on a complex method, which has been continually improved in the last decades. One way to ensure the quality of these data is to measure the same CO_2 fluxes using different and independent methods and test whether or not the estimates are similar. In this study, we measured the amount of CO_2 emitted at night by a forest and its soil, using two different techniques. We found that, overnight, the time course of the measurements diverged. Further analysis showed that this difference could not be explained by biological mechanisms. Thus, there may be an error in the flux tower measurements of the CO_2 emitted by the forest, owing to unaccounted-for physical processes. We discussed what implication this measurement error has on the use of these data, and what future steps should be taken by the community to identify and correct this error.

Keywords: Eddy covariance, soil respiration, ecosystem respiration, partitioning, temperature sensitivity

1 Introduction

Ecosystem respiration (R_{eco}), the second largest flux in the terrestrial carbon cycle after gross primary productivity (Friedlingstein et al., 2019), is challenging to quantify in tall canopy ecosystems, such as forests. Indirect, bottom-up approaches consist of separately measuring respiration components (soil, leaf and stem), scaling-up in space using structural information (bare ground area, stem area, leaf area), and eventually scaling-up through time using responses to drivers (Law et al., 1999; Ohkubo et al., 2007; Wang et al., 2017). The direct, top-down estimation method (eddy-covariance) is based on solving an equation of conservation of CO_2 mass in a volume, to infer the net ecosystem exchange of CO_2 (NEE) between an ecosystem and the atmosphere. This method measures R_{eco} only during night-time, when there is no photosynthesis, as the sum of vertical turbulent flux (F_{CT}) and change in storage (F_{CS}) in a control volume (Aubinet et al., 2012). These night-time measurements are used in combination with different sets of environmental drivers to estimate daytime R_{eco}, in order to quantify the total ecosystem CO_2 loss, allowing estimation of gross primary production (GPP = NEE - R_{eco}) (Reichstein et al. 2005; Moffat et al. 2007; Lasslop et al. 2010). However, night-time measurement of R_{eco} from flux towers has been a longstanding challenge because of weak turbulence and advection leading to a potential bias in night data (Aubinet et al., 2010; Aubinet et al., 2000; Belcher et al.,2012; Hayek et al., 2018; Leuning et al., 2008; Van Gorsel et al., 2011; Van Gorsel et al., 2007).

Most common methods of estimating daytime R_{eco} rely on the following assumptions: (1) the response of R_{eco} to drivers is similar between day and night, (2) the observed response of night R_{eco} can be extrapolated to a range beyond the measurements (e.g. a common issue is that air temperature (T_{air}) is higher during the day than during the night), and (3) the apparent temperature sensitivity estimated over a large time window (e.g., weeks) can be used to estimate short-term temperature sensitivity (e.g., hours). Moreover, R_{eco} estimation may also be biased from poorly constrained relationships (noisy data or biased relationship, e.g. due to a systematic error leading to under-estimated measurements in specific environmental conditions or time of day), invalid assumptions (e.g. different R_{eco} mechanisms occurring during the day vs. during the night) or incorrect algorithms (Desai et al., 2008).

The contribution of multiple respiratory sources to R_{eco}, all responding at different temporal and spatial scales to a range of different drivers, makes testing these assumptions complex. Aboveground CO_2 efflux (R_{AG}) results from the dynamic regulation of plant physiological processes occurring in leaves, branches, and stems in a way that interacts with environmental drivers such as temperature. For instance, leaf respiration is known to acclimate seasonally to temperature, with a higher short-term (hours to days) temperature sensitivity compared to long-term apparent temperature sensitivity (days to months) (Aspinwall et al., 2016; Atkin et al., 2000; Crous et al., 2011; King et al., 2006). Leaf respiration is also known to be inhibited by light (Crous et al., 2012; Crous et al., 2011; Heskel et al., 2013; Kok, 1949; Way et al., 2019). This dynamic physiological regulation of leaf respiration calls into question the validity of estimating daytime R_{eco} from night-time measurements (Keenan et al., 2019; Wehr et al., 2016).

R_{soil} has been measured continuously at an increasing number of sites (Bond□Lamberty et al., 2020) and can provide a check of consistency for eddy-covariance based R_{eco} estimates, because $R_{eco} = R_{soil} + R_{AG}$. This constraint indicates that R_{eco} should be larger in absolute magnitude compared to R_{soil}, and the difference in temporal dynamic between R_{eco} and R_{soil} should be a result of the R_{AG} temporal dynamic (Barba et al., 2018; Phillips et al., 2017; Wang et al., 2017). However, mismatches between such bottom-up approaches and direct R_{eco} estimates are common (Giasson et al., 2013; Phillips et al., 2017; Speckman et al., 2015; Thomas et al., 2013). These uncertainties may arise from different measurement footprints or spatial scales, as the spatial resolution of R_{soil} is much smaller than R_{eco} (~ 0.01 m^2 vs. ~ 1 km^2, a scaling factor of 10^6), and the time resolution of the measurements also differs (2-5 minutes of sampling for R_{soil} and 30-60 minutes for R_{eco}). R_{soil} is subject to measurement errors, which are mostly random (Cueva et al., 2015; Heinemeyer et al., 2007; Pumpanen et al., 2004), but may be systematic, e.g., in a closed chamber system, if there is a volume error. Furthermore, R_{soil} estimates are often clustered at a location due to power and tubing limitations. In contrast, R_{eco} measurements may be affected by a systematic error or bias, and have large random error, following a double exponential distribution (Hollinger & Richardson, 2005).

Heterotrophic respiration (R_{hetero}) models have often been applied to estimate R_{soil} and R_{eco} (Lloyd & Taylor, 1994; Reichstein et al., 2005), because R_{hetero} represents a large proportion of R_{soil}, which represents a large proportion of R_{eco}. Moreover, these fluxes have common drivers: temperature and soil moisture, albeit on different components, e.g. soil temperature, air temperature, stem temperature, leaf temperature. Lloyd and Taylor (LT) describes the temperature sensitivity of heterotrophic respiration at a given soil moisture (Lloyd & Taylor, 1994), and has been commonly used in eddy-covariance R_{eco} temporal gap-filling. The Dual Arrhenius and Michaelis Menten (DAMM) model (Davidson et al., 2012) is a semi-mechanistic heterotrophic respiration model which includes regulation of substrate availability via soil water content limitation in dry soils and oxygen limitation in wet soils. It has been previously applied to R_{soil} (Drake et al., 2018), and has been used in a data-model synthesis study to improve estimations of R_{eco} (Sihi et al., 2018). An increasingly popular method to modeling R_{eco} and R_{soil} is machine learning, such as Artificial Neural Networks (ANN) (Moffat et al., 2007), which allow the use of many drivers and results in good fitting quality, but cannot be interpreted mechanistically.

Reconciling measurements of soil respiration with ecosystem respiration is an important step toward resolving the long-standing challenge of using night-time NEE measurements and estimates of daytime R_{eco} to quantify total R_{eco} (Aubinet et al., 1999; Van Gorsel et al., 2007), and hence to improving accuracy of GPP estimation. The main aim of this study is to decipher what we can learn from concurrent measurements of R_{eco} and R_{soil}, at diurnal (night-time for R_{eco}) and seasonal time scales, and what needs to be studied further. We had the following objectives:

1) To analyse the diurnal (night-time for R_{eco}) and seasonal dynamics of R_{eco} and R_{soil}, and evaluate their responses to environmental drivers of soil and air temperatures and soil water content over a range of time scales from half-hourly to seasonal.
2) To evaluate whether measurements of R_{soil} can inform predictions of R_{eco} based on the Lloyd and Taylor model, the DAMM model, and machine learning.

2 Materials and methods

2.1 Site description

The Cumberland Plain Terrestrial Ecosystem Research Network (TERN) OzFlux site (Fluxnet code: AU-Cum), located near Sydney, Australia (latitude: – 33.61518; longitude: 150.72462), is a mature dry sclerophyll woodland, with a canopy of various aged trees and up to 25 m in height composed of two main species, *Eucalyptus moluccana* and *E. fibrosa*, a mid-canopy dominated by *Melaleuca decora* and an understory dominated by the shrub *Bursaria spinosa* and various other shrubs, forbs, grasses and ferns. This site is equipped with a 30 m tall eddy-covariance tower with instruments at the 29 m height measuring net ecosystem exchange of CO_2 (NEE).

Soil respiration was measured at the EucFACE study site, within the same patch of mature dry sclerophyll woodland, approximately 1.4 km from the flux tower (Figure S1). This site was selected because of its proximity and ecological similarity to the flux tower footprint, and availability of AC power required for running the autochambers. The EucFACE and flux tower sites are both dominated by the Shale Gravel Transition Forest plant community (Tozer, 2003) and share a similar disturbance history (no fire in >20 years). Furthermore, standing aboveground biomass at both sites was approximately 4700 g C m^{-2}, and total net primary production was also similar, at about 600 g C m^{-2} (Table S1). However, the canopy at EucFACE is dominated by *E. tereticornis*, with an understory dominated by various shrubs, forbs, and the C3 grass, *Microlaena stipoides*. EucFACE was equipped with three auto-chambers measuring R_{soil} (see section 2.4 for details on R_{soil} measurements).

During the 4-year period 2014-2017, the mean annual precipitation was 856 mm yr^{-1} and the mean T_{air} was 18.5 □. Soil C stocks were similar at about 60 T ha^{-1}, but EucFACE soil was sandier than at the flux tower (Table S2).

2.2 Meteorological drivers

At the flux tower site, meteorological drivers of air temperature (T_{air}), soil temperature (T_{soil}), and soil water content (θ), were measured at half-hourly resolution. T_{air} was measured using a HMP45C (Vaisala, Vantaa, Finland) sensor at 29 m height. T_{soil} was measured within 20 m of the flux tower using an averaging thermocouple buried at 3 cm and 7 cm depths (model TCAV, Campbell Scientific,

Logan, UT, USA). θ was monitored at 5 cm depth using a CS616 probe (Campbell Scientific, Logan, UT, USA) installed horizontally.

At EucFACE, T_{soil} and θ were measured at three locations, within 1 m of auto-chambers measuring R_{soil}. T_{soil} and θ were measured every 15 minutes using a time-domain reflectometry probe (CS650-L; Campbell Scientific, Logan, UT, USA), and then averaged to 30 minutes to match the eddy-covariance timestamps. The 30 cm-long probe was inserted at 45° in the soil at the surface, measuring θ at 0 to 21 cm depth, and T_{soil} at 5 cm depth.

Rainfall was measured every half-hour using a tipping bucket (Tipping Bucket Rain gauge TB4; Hydrological Services Pty Ltd, Liverpool, NSW, Australia).

2.3 R_{eco} data

2.3.1 Night-time R_{eco} observations

R_{eco} was measured at night (sunset to sunrise) as:

$$R_{eco} = F_{CT} + F_{CS} \quad (1)$$

where F_{CT} is the vertical turbulent exchange of CO_2 (eddy-covariance method, (Baldocchi, Hicks, & Meyers, 1988)), and F_{CS} is the change in storage of CO_2 within the canopy. The eddy covariance system included a CSAT 3D sonic anemometer (Campbell Scientific, Inc., Logan UT) and a Li-7500A infrared gas analyser (IRGA, LI-COR, Inc., Lincoln, NE, USA). The processing of high-frequency data to calculate F_{CT} was done with the EddyPro® open source software (LI-COR, Inc., Lincoln, NE, USA), keeping data that passed quality control (qc = 0 or qc = 1) tests for stationarity and turbulence development (Foken et al., 2004) and met adequate signal strength for the infrared gas analyser (Renchon et al., 2018). The calculation of F_{CS} was done using a profiler system that measured CO_2 at eight heights (Renchon et al., 2018); data were discarded if any of the inlets was not working. No clear friction velocity (u_*) threshold was found at the site (Figure S2; R_{eco} was independent of u_* for a variety of T_{air} and θ bins), so a u_* threshold was not applied. We further filtered out outliers, defined as data points above the 95% quantile (9.9 μmol m^{-2} s^{-1}) and below the 5% quantile (-3.3 μmol m^{-2} s^{-1}) of quality controlled data.

After applying these quality checked criteria, we were left with 15,686 R_{eco} observations over the 4-year period 2014-2017, out of a potential of 35,271 half-hourly night data (~45% of potential night data was kept). Of total night data, 17% had missing F_{CS} (mostly a dead pump), 17% had poor IRGA signal strength, 29% did not pass the F_{CT} stationarity and turbulence development quality check (qc = 2).

2.3.2 Half-hourly R_{eco}

To construct a continuous time series, missing half-hourly R_{eco} night-time data were filled using an artificial neural network (using Levenberg-Marquardt algorithm and 15 hidden layers) built on high quality data (when F_{CT} qc = 0 or 1, signal strength is above threshold, and F_{CS} is available), with T_{air} and θ as drivers at the flux tower site (Figure S3).

2.3.3 Nightly R_{eco}

We generated a nightly (i.e. one data point per day, representing night-time R_{eco}) estimate of R_{eco} dataset by first estimating nightly R_{eco} as the median of night half-hourly observations of R_{eco}, when at least 10 high quality observations of F_{CT} plus F_{CS} were available for a night (without using gap-filled half-hourly data). Then, if F_{CS} was missing, but at least 10 half-hourly observations of F_{CT} were available, nightly R_{eco} was filled using an artificial neural network with nightly R_{eco} as target and F_{CT}, T_{soil}, θ, R_{soil}, and u_* as drivers ($r^2 = 0.67$). If both F_{CS} and F_{CT} were missing, or <10 F_{CT} half-hourly observations were available, nightly R_{eco} was filled using an ANN with nightly R_{eco} as target and T_{soil}, θ, and R_{soil} as drivers ($r^2 = 0.50$).

2.4 R_{soil} data

2.4.1 Observations

We measured R_{soil} using automated chambers (20-cm diameter chamber, LI-8100-104 model and LI-8100A IRGAs, LI-COR Environmental, Lincoln, NE, USA) at three different locations at EucFACE. The IRGAs measured CO_2 concentration during 4.5 minutes, with a 30-s deadband and a postpurge, every half-hour during the 4-year period 2014-2017. The dataset of R_{soil} for 2014 and 2015 was previously published (Drake et al., 2018). The raw data were qc checked with a threshold criterion of

coefficient of variation (CV < 1.3) and coefficient of determination of the fit ($r^2 > 0.97$). Due to mechanical issues, data collection was interrupted during some periods. In total, during the 4 year period, we collected 133 823 quality checked R_{soil} observations, out of a potential total of 210 384. We kept 64 % of the data, 36 % were missed due to mechanical interruption or qc check. From chamber one to chamber three, we collected 74 %, 63 %, and 53 % of potential data, respectively.

2.4.2 R_{soil} gap-filling

In order to evaluate the utility of R_{soil} in predicting R_{eco} using an artificial neural network (see 2.6), we produced a continuous dataset of R_{soil}, by gap-filling the data for each of the three chambers separately, using the semi-mechanistic DAMM model (Davidson et al., 2012; Drake et al., 2018). The DAMM model is composed of a maximum potential rate of R_{soil}, V_{max}, which is an exponential function of soil temperature, which is then potentially limited by the availability of C substrate (MM_{Sx}) or by oxygen (MM_{O2}). Those two limiting terms vary between 0 and 1, and are dependent on θ.

$$R_{soil} = V_{max}\, MM_{Sx}\, MM_{O2} \quad (2)$$

where V_{max} is a function of activation energy and soil temperature;

$$V_{max} = \alpha_{Sx}\, e^{-E_a/RT_{soil}} \quad (3)$$

where α_{Sx} is a pre-exponential factor (mg C cm^{-3} h^{-1}), Ea is the activation energy (kJ mol^{-1})), R is the universal gas constant (8.314 J mol^{-1} K^{-1}), and T_{soil} is soil temperature in Kelvin (°K).

MM_{Sx}, the availability of C substrate, is a function of θ (m^3 m^{-3}).

$$MM_{Sx} = \frac{[S_x]}{kM_{Sx} + [S_x]} \quad (4)$$

$$[S_x] = [S_{xsoluble}]\, D_{liq}\, \theta^3 \quad (5)$$

$$[S_{xsoluble}] = p\, [S_{xtotal}] \quad (6)$$

where kM_{Sx} is a Michaelis constant (g C cm^{-3}), $[S_{xsoluble}]$ is the amount of C substrate potentially soluble, which we assume to be a fraction (p = 0.024) of total soil C ($[S_{xtotal}]$= 0.0125 g cm^{-3}) (Drake

et al., 2018), and D_{liq} is a diffusion coefficient of the substrate in liquid phase (D_{liq} = 3.17, dimensionless).

MM_{O2}, the oxygen limitation factor, is also a function of θ.

$$MM_{O2} = \frac{[O_2]}{kM_{O2} + [O_2]} \quad (7)$$

$$[O_2] = D_{gas}\, O_{2_{airfrac}}\, a^{4/3} \quad (8)$$

$$a = 1 - \frac{D_b}{D_p} - \theta \quad (9)$$

where $[O_2]$ is oxygen concentration, kM_{O2} is the Michaelis constant for O_2 (L L^{-1}), D_{gas} is the diffusion coefficient for O_2 in the air (D_{gas} = 1.67, dimensionless), $O_{2airfrac}$ is the volume of O_2 in the air ($O_{2airfrac}$ = 0.209 L L^{-1}), a is the air-filled soil porosity, D_b is soil bulk density (D_b = 1.53 g cm^{-3}) and D_p is particle density (D_p = 2.52 g cm^{-3}).

R_{soil} is then converted from mg C cm^{-3} hr^{-1} to the same units as the R_{eco} measurements (μmol CO_2 m^{-2} s^{-1}) following:

$$R_{soil2} = 10^4\, Soil_{depth}\, R_{soil}/10^3/12 \times 10^6/60/60 \quad (10)$$

where $Soil_{depth}$ is the effective soil depth (10 cm).

For each chamber, we fitted the DAMM model (R_{soil2} fitted to four parameters: αsx, E_a, kM_{Sx} and kM_{O2}) to all the available quality checked data. We then obtained three parameter sets for the model (four parameters for each of the three collars). We then used the model to fill the gaps for each chamber, using their respective parameter sets. Finally, we calculated the average from the three locations, using quality checked observations when available or chamber-specific gap-filled estimates when observations were not available (Figure S2). We note that the gap-filled R_{soil} values have a lower range than the observations, and that this contributes to uncertainty and potential bias in the R_{soil}-based ANN estimates of R_{eco}.

2.5 Seasonal and diurnal apparent temperature sensitivity

We estimated the apparent temperature sensitivity of night-time observations (i.e., no gap-filled data) of R_{eco} and R_{soil} (based on both T_{air} and T_{soil}) by fitting an equation (Lloyd & Taylor, 1994) on monthly averages (seasonal apparent temperature sensitivity) and hourly averages (hourly apparent temperature sensitivity). The Lloyd & Taylor equation was firstly developed to describe R_{soil} and later applied to R_{eco} (Desai et al., 2008).

$$R = R_{10} e^{E_0\left(\frac{1}{10+46.02} - \frac{1}{T+46.02}\right)} \quad (13)$$

where R is either R_{soil} or night-time-R_{eco}; R_{10} is the basal respiration parameter fitted to data normalized to 10 □, E_0 is the activation energy parameter fitted on data, defining the steepness of the curve, and T is either T_{soil} or T_{air}. Temperature sensitivities were calculated only when concurrent observations of R_{eco} and R_{soil} were available.

2.6 Alternate predictions of R_{eco} using R_{soil}

We used an artificial neural network (Moffat et al., 2007) to model R_{eco} as a function of drivers: T_{soil}, T_{air}, θ, and R_{soil}. We used MATLAB R2019b with the Levenberg-Marquardt algorithm, 15 hidden layers, and trained the network on 75% of the target data. First, we created four ANN, with the following combinations of drivers: 1) T_{air}, 2) T_{soil}, 3) T_{soil} and θ, and 4) T_{soil}, T_{air} and θ. Then, we created four more ANN by adding half-hourly, gapfilled R_{soil} to these drivers. We give the r^2 and RMSE (residual mean square error) of the fits.

3 Results

During the four-year period 2014-2017, the mean annual precipitation was 856 mm yr^{-1} and the mean T_{air} was 18.5 □. On average, precipitation was higher in summer (December through February, 289 mm) than winter (June through August, 187 mm), but precipitation was aseasonal, with dry periods and wet periods throughout. At EucFACE, T_{soil} had a low variability across the three sensors, as compared to θ and R_{soil} (Figure 1c, grey shade barely visible). Average night-time T_{soil} varied between 10 □ (6 July 2015) and 27 □ (12 February 2017), and was slightly higher at flux tower site than at EucFACE, possibly due to sensor differences (Figure 1c). The soil dried faster after rainfall events at the flux tower, and had a higher minimum (0.07 m^3 m^{-3} for the flux tower site, 0.02 m^3 m^{-3} for EucFACE), probably as a result of sensor depth (5 cm at the flux tower site, 0-21 cm at EucFACE) and soil texture (more clay at the flux tower site, sandier at EucFACE) (Figure 1b, Table S2). At EucFACE, across the three R_{soil} locations, θ had a large spatial variability (Figure 1b, grey shade), with different locations drying faster after rain events, probably due to spatial variation in soil properties (Figure 1b, black dots and grey shade). Median nightly R_{soil} ranged from 1.4 μmol m^{-2} s^{-1} on average in winter to 3.5 μmol m^{-2} s^{-1} in summer, while median nightly R_{eco} ranged from 2.0 μmol m^{-2} s^{-1} in winter to 4.6 μmol m^{-2} s^{-1} in summer (Figure 1a). R_{eco} and R_{soil} had a similar seasonal time dynamic, with R_{eco} being higher than R_{soil} (Figure 1a). R_{soil} had a large variability in warm, moist conditions (Figure 1a, grey shade shows range across the three sample locations at the EucFACE site).

We used monthly and hourly median values of concurrent, observed data (no gap-filling) to evaluate seasonal and diurnal patterns, respectively, for all four years combined. R_{eco} and R_{soil} had a similar seasonal pattern and followed the seasonal pattern of T_{air} and T_{soil} (Figure 2a, Figure 3a,c). R_{eco} - R_{soil} (presumably, R_{AG}) had a lower seasonal amplitude compared to R_{eco} and R_{soil}, but also peaked in summer months (Figure 2a, Figure 3e). T_{soil} and T_{air} both reached maximum values around 15.00 hrs and minimum around 6.00 hrs, but the diurnal amplitude of T_{air} was much larger than diurnal amplitude of T_{soil} (2.3 □ for T_{soil} and 8.0 □ for T_{air}) (Figure 2b). Note that because Figure 3a values were monthly medians of night-time observations, T_{soil} was higher than T_{air}. R_{soil} was relatively flat diurnally, with a diurnal amplitude of 0.28 μmol m^{-2} s^{-1} with an average R_{soil} rate of 2.4 μmol m^{-2} s^{-1}

(Figure 2b, Figure 3b). R_{eco} had a large amplitude over the available observation range (19.00 hrs to 6.00 hrs), with an amplitude of ~ 1.8 μmol m^{-2} s^{-1} and an average R_{eco} rate of ~ 2.7 μmol m^{-2} s^{-1} (Figure 2b, Figure 3d). As a result, R_{eco} - R_{soil} had a large diurnal (overnight) amplitude (Figure 2b, Figure 3f). Seasonality of individual years are shown in Figure S4, and diurnal patterns of individual months in 2017 are shown in Figure S5.

The apparent temperature response differed between seasonal and diurnal time resolution, as shown by comparisons of fits to the Lloyd and Taylor (1994) model, driven only by temperature (T_{soil} or T_{air}). For R_{soil}, the seasonal apparent temperature response was higher than the diurnal apparent temperature response (Figure 3a, b), and the temperature sensitivity (E_0) parameter was unrealistically low when R_{soil} was fit to T_{air} (Table 1). For R_{eco}, the seasonal apparent T_{soil} and T_{air} responses produced reasonable parameters, but the diurnal apparent T_{soil} response was unrealistic (Figure 3c, d, Table 1). For R_{eco} - R_{soil}, the seasonal apparent response parameters were reasonable, whereas the diurnal apparent temperature responses were not, with E_0 values far too high and R_{10} values too low (Figure 3e, f, Table 1).

We used the semi-mechanistic DAMM model to compare how R_{soil} and R_{eco} responded to the combined influence of temperature and soil moisture. Fitting nightly median and half-hourly R_{soil} observations using the semi-mechanistic heterotrophic respiration DAMM model yielded r^2 above 0.5 (half-hourly: r^2 = 0.60, RMSE = 0.86 μmol m^{-2} s^{-1}; night median: r^2 = 0.66, RMSE = 0.79 μmol m^{-2} s^{-1}. Figure 4, Table 2). Fitting nightly median R_{eco} yielded an r^2 of 0.50, and a RMSE of 1.05 μmol m^{-2} s^{-1}, but the fit quality was much lower against half-hourly observations (R_{eco}: r^2 = 0.10, RMSE = 2.43: Figure 4, Table 2).

The DAMM model parameters for R_{eco} differed from R_{soil}: kM_{SX} was higher for R_{eco} (i.e. more substrate limitation at low θ for R_{eco}), and kM_{O2} was lower for R_{eco} (i.e. more oxygen limitation at high θ for R_{eco}) at both time scales, in other words, R_{eco} was more limited by θ than R_{soil} (Figure 4, Table 2). Interpretations of α_{Sx} and Ea are difficult due to the equifinality of those parameters.

We compared performance of the LT, DAMM and ANN models of R_{eco}, with and without R_{soil} as a driver. Predictions of R_{eco} based on half-hourly observations were poor for all three models, with r^2 below 0.13 and RMSE above 2.4 μmol m^{-2} s^{-1}, but the predictions of daily R_{eco} (night median) were much more accurate (Table 3), with r^2 up to 0.58 and RMSE about 1 μmol m^{-2} s^{-1}. The ANN model including R_{soil} together with T_{air}, T_{soil} and θ predicted night-time R_{eco} better than other models tested (Table 3). Using R_{soil} to inform ANN to constrain estimates of R_{eco} slightly improved estimates of R_{eco}; r^2 increased by up to 0.02 at the half-hourly scale and by 0.13 on a daily scale (Table 3). The DAMM model predicted R_{eco} with similar performance as the best ANN models, whereas the LT model performed worse than models that incorporated θ (Table 3). On a daily time scale resolution, the LT model fits resulted in r^2 values of up to 0.39 (with T_{soil}) and the r^2 for the DAMM model was 0.50.

4 Discussion

4.1 Spatial variability of R_{eco} and R_{soil} and challenges for scaling

In this study, R_{soil} and R_{eco} were measured in similar contiguous forest stands with similar soil types, yet spatial variability of ecosystem properties and processes within the flux tower footprint and among the soil respiration chambers must be considered in interpreting our results. The spatial heterogeneity of R_{soil} may not have been fully captured by the use of three autochambers and the few sample locations at EucFACE precluded characterisation of a spatially integrated value of R_{soil} that would reflect fluxes detected by the tower measurements. We note that there is often a tradeoff between R_{soil} sampling frequency and the number of locations where it can be measured (Savage & Davidson, 2003). Nevertheless, an earlier study at EucFACE compared manual biweekly sampling at 48 soil collars with continuous (half-hourly) measurements on six autochambers (including the elevated CO_2 treatment which was not included in this study), and found very similar flux rates across the EucFACE experimental site (Drake et al., 2018). Moreover, the variability of vegetation and soil properties within the flux tower footprint should also be considered, although NEE did not differ significantly between sandy and clayey stands (Griebel et al., 2020). Therefore, we expect spatial heterogeneity within the flux tower footprint to contribute at least as much variability to R_{eco} fluxes as differences in ecosystem properties between the flux tower and EucFACE.

We avoided comparing magnitude of fluxes, and focused mainly on temporal patterns instead, to avoid over-interpreting the results. We acknowledge that some of the inconsistencies in estimating R_{AG} might be attributable to a mismatch of both scale and heterogeneity in locations of the R_{soil} and R_{eco} measurements. Nevertheless, we contend that our analyses of the temporal patterns and environmental drivers are reasonable, as these two sites are very close in space (Fig. S1), and have similar vegetation, biomass and NPP (Table S1), soil properties (Table S2) and climate (Figure 1). Further research to evaluate the drivers of spatial variability in R_{soil} should demonstrate how to enhance the representativeness of sampling design (Mitra et al., 2014).

4.2 Seasonal and diurnal patterns of R_{soil}, R_{eco} and implications for R_{AG}

In this study, in a warm-temperate, mature eucalypt woodland, the observed diurnal pattern of R_{soil} was relatively flat while the observed overnight diurnal pattern of R_{eco} varied. This result challenges the idea that R_{soil} can be used as a proxy of the diurnal pattern of R_{eco}. In an influential paper (Reichstein et al., 2005), the diurnal amplitude of observed R_{soil} was compared to the diurnal amplitude of R_{eco} estimated with different methods, validating the methods with similar estimated R_{eco} and measured R_{soil} diurnal amplitudes. However, this method should be questioned if R_{eco} and R_{soil} have different diurnal amplitudes at other sites. In another important paper (Desai et al., 2008), it was highlighted that emerging datasets of automated soil chambers will help to quantify diurnal trends of soil respiration, suggesting they should explain most diurnal trends of ecosystem respiration. However, R_{soil} observations have not yet provided a consistent constraint on R_{eco}.

Because the large overnight amplitude of R_{eco} cannot be explained by diurnal patterns of R_{soil} at the Cumberland Plain site, either R_{AG} has to make up the difference, by decreasing strongly as T_{air} declines (Drake et al., 2019), or observations of R_{eco} and/or R_{soil} are biased. The unrealistically high apparent temperature sensitivity relationships for ($R_{eco} - R_{soil}$) shown in Table 1 suggest that R_{AG} is not the primary contributor to the large amplitude of night-time R_{eco} (Desai et al., 2008; Reichstein et al., 2005). Direct measurements of eucalypt canopy respiration in whole-tree chambers suggest that the short-term Q_{10} of R_{AG} is approximately 2.2 (Drake et al., 2016), with R_{10} values expressed on a canopy leaf area basis close to 0.5 μmol m^{-2} s^{-1} and remaining above 0.3 μmol m^{-2} s^{-1} even below 5°C (Drake et al., 2019). For these reasons, we conclude that R_{AG} does not contribute to the majority of the difference between R_{eco} and R_{soil}, suggesting that a bias in night-time R_{eco} and/or R_{soil} measurements are responsible for the unrealistic R_{AG} estimates (Hayek et al., 2018; Van Gorsel et al., 2007). We cannot rule out the possible contribution of spatial heterogeneity to the diurnal difference between R_{eco} and R_{soil}, but further investigations into this issue are beyond the scope of this study. Rather, we explore the contribution of R_{eco} to the unrealistic diurnal dynamics in the following sections.

4.3 Bias of night-time and daytime R_{eco} by standard methods?

4.3.1 Night-time estimates of R_{eco}

A known problem of eddy-covariance is the assumption of horizontal flux (also named advection flux) being negligible in the mass balance (see Equation 1). For this assumption to be reasonable, the standard method is to filter out data when advection is assumed to be important. This method is called u_* filter method (Aubinet et al., 2000), and relies on the idea that night-time NEE should not depend on friction velocity, since it is not a driver for ecosystem respiration. It is usually observed that NEE within a narrow range of temperature and soil moisture increases or decreases with u_* at values below a certain threshold. This threshold can be determined with an algorithm such as the change point detection method (Barr et al., 2013). Data below this threshold should be discarded and then gap-filled. Without applying this method, night-time R_{eco} would usually be under-estimated, as advection typically leads to loss of CO_2 (but not always). Studies still question if this method is reliable and suggest alternative methods, such as using early night data only (3 hours after sunset (Van Gorsel et al., 2007)), or using intercept of light response from daytime data (Lasslop et al., 2010), or attempting to quantify a missing flux from storage measurements and advection (Hayek et al., 2018).

At the Cumberland Plain site, there was no clear dependence of night-time NEE with friction velocity (Figure S2), and thus filtering and gap-filling night-time data at low u_* (usually u_* below ~ 0.2 m s^{-1} is filtered out) did not change integrated R_{eco} (Figure S6). This result could mean that there is no advection at the flux tower site, or that advection occurred but was not dependent on u_*. R_{eco} was, however, much larger early in the night compared to late at night, as shown in Figure 2b, and this high early-night NEE was mostly the result of high F_{CS}, as F_{CS} decreased overnight while F_{CT} remained relatively flat (Figure S7). Also, F_{CS} was larger than F_{CT} in magnitude. This result highlights the importance of F_{CS} in capturing both the magnitude and pattern of R_{eco} at night. As a result, using data from 3 hours after sunset did change the annual budget of R_{eco} from 1300 g C m^{-2} yr^{-1} on average when using all night data, to 1520 g C m^{-2} yr^{-1} on average when using only three hours after sunset. The importance of storage and advection fluxes is known to vary from site to site; although advection

is usually low at sites such as ours with low slope (Aubinet et al., 2005), it can remain important at such sites (McHugh et al., 2017).

4.3.2 Daytime estimates of Reco

Daytime R_{eco} is often inferred from the apparent temperature response of night-time NEE, assuming that R_{eco} night-time temperature response is similar to its daytime response. Using stable isotopes, Wehr et al. (2016) showed that the standard LT temperature response method over-estimated daytime R_{eco}. The authors of the study suggested that the mismatch was likely caused by light inhibition of leaf respiration (Wehr et al., 2016). Light inhibition could cause an over-estimation of daytime R_{eco} by up to 25% as compared to standard methods (T. Keenan et al., 2018; T. F. Keenan et al., 2019). Our analysis suggests another possibility causing an over-estimation of daytime R_{eco}. The apparent temperature response of R_{eco} may result from a systematic bias, as advection may co-vary with temperature, both decreasing overnight. This artefact would result in an over-estimation of daytime R_{eco} even without inhibition of leaf respiration, and must be considered. Improved atmospheric measurements and analytical methods are becoming more widely available (Hayek et al., 2018), which should reduce errors related to unaccounted-for storage or advection fluxes.

Our results show that better understanding of above-ground respiration is required to reconcile R_{eco} and R_{soil}, particularly over diurnal time scales (Vargas, Carbone, Reichstein, & Baldocchi, 2011). The seasonal contribution of R_{eco} components has been estimated using low time resolution measurements (monthly) or using modelling (Law et al., 1999), but to our knowledge no study has attempted to measure continuously all R_{eco} components as the relative contribution of R_{soil}, stem respiration (R_{stem}) and leaf respiration (R_{leaf}) to R_{eco} at hourly temporal resolution. Such an analysis would be invaluable to reconcile estimates of daytime ecosystem respiration and quantify the potential over-estimation of R_{eco} by failing to account for daytime light inhibition of R_{leaf}. For example, if R_{leaf} represents 10% of R_{eco}, and light inhibition of R_{leaf} was 60% (Way et al., 2019), light inhibition can only reduce daytime R_{eco} by 6%. Moreover, R_{soil}, R_{stem}, and R_{leaf} respond to different temperatures (soil temperature, stem temperature and leaf temperature) and are lagged in time, and thus have distinct diurnal patterns.

Improving understanding of component contributions to diurnal patterns of R_{eco} will improve ecosystem models, with important consequences for estimating ecosystem C uptake.

4.4 Modelling R_{eco} using the DAMM model

The efficacy of the DAMM model for estimating R_{eco} at a daily time step encourages the use of this or similar semi-mechanistic models for eddy-covariance gap-filling and also for R_{eco} models, as it has the advantage of being interpretable and is thus more insightful than a neural network (Richardson et al., 2006). The LT model is based only on temperature, albeit fitted to 15-day windows it incorporates some implicit moisture dependency (Reichstein et al. 2005).

Toward the goal of reconciling seasonal and diurnal patterns of R_{eco} and R_{soil}, more understanding of respiration components of R_{eco} is required. Fitting mechanistic models to R_{eco} can be insightful to make progress in that area. Although DAMM was developed for heterotrophic respiration (Davidson et al. 2012), it has been applied to total soil respiration (e.g., Drake et al. 2018), because the response of R_{soil} to T_{soil} and θ is similar to the heterotrophic respiration response to these drivers as heterotrophic respiration contributes to a large proportion of R_{soil} and R_{eco}, and autotrophic respiration responses are similar, i.e. exponential temperature response, limited by θ. Applying DAMM to R_{eco} assumes that most of the flux is derived from soil, although we recognize that stem and leaf respiration respond to different drivers. The advantage of fitting LT on a 15-day moving window is to distinguish the short-term from the long-term temperature sensitivity, whereas DAMM has the advantage of better capturing the response of R_{eco} to changing soil moisture. Nevertheless, none of the empirical models developed to date for estimating daytime R_{eco} has realistically incorporated the responses of inferred R_{AG} to changing temperature or soil moisture, leaving a gap in understanding and predicting the full carbon balance of ecosystems.

5 Conclusion

Our concurrent half-hourly measurements of ecosystem and soil respiration in a mature eucalypt woodland showed a similar seasonality for R_{eco} and R_{soil} over the four-year period, suggesting that R_{soil} drives the seasonality of R_{eco}. By contrast, the averaged diurnal variations were much larger for R_{eco} than for R_{soil}, implying that aboveground respiration drives the diurnal patterns of R_{eco}. However, the apparent temperature sensitivity of R_{eco} and especially ($R_{eco} - R_{soil}$) was unrealistically high, indicating that a systematic bias in the measurements of R_{eco} at night might be leading to an underestimation of R_{eco} later during the night. This bias, of decreasing R_{eco} with overnight cooling, was not correctable by u_* filtering and storage fluxes estimated from a profiler system. The unrealistically high apparent temperature sensitivity of night-time R_{eco} would propagate into over-estimates of daytime R_{eco}, and thus also overestimate GPP resulting from common partitioning methods. The u_* filtering method is likely to be insufficient for many sites, due to missing storage or advection flux biases. More importantly, NEE and night-time R_{eco} would remain under-estimated without correction for this systematic bias, regardless of the partitioning method. Clearly, more detailed measurements of component respiration fluxes in addition to soil respiration, and appropriate scaling algorithms, are required for improved predictive understanding of ecosystem carbon cycling.

Code and data availability

All the datasets and scripts used in this manuscript can be downloaded at: **https://doi.org/10.6084/m9.figshare.12357449.v1**. Soil respiration data was also contributed to the COSORE database (Bond□Lamberty et al., 2020).

Author contributions

AAR and EP conceived of the project; AAR, EP, JED, and CM collected the data and ran the experiment; AAR analysed the data; AAR wrote the manuscript with input from all other authors.

Competing interests

The authors declare that they have no conflict of interest.

Acknowledgements

This work was supported by the Australian Research Council (DP170102766) and the Australian Terrestrial Ecosystem Research Network, as part of the National Cooperative Research Infrastructure System. EucFACE was built as an initiative of the Australian Government as part of the Nation-building Economic Stimulus Package, and is supported by the Australian Commonwealth in collaboration with Western Sydney University. We gratefully acknowledge technical support by CVM Barton, V Kumar, A Griebel, C McNamara, and D Metzen.

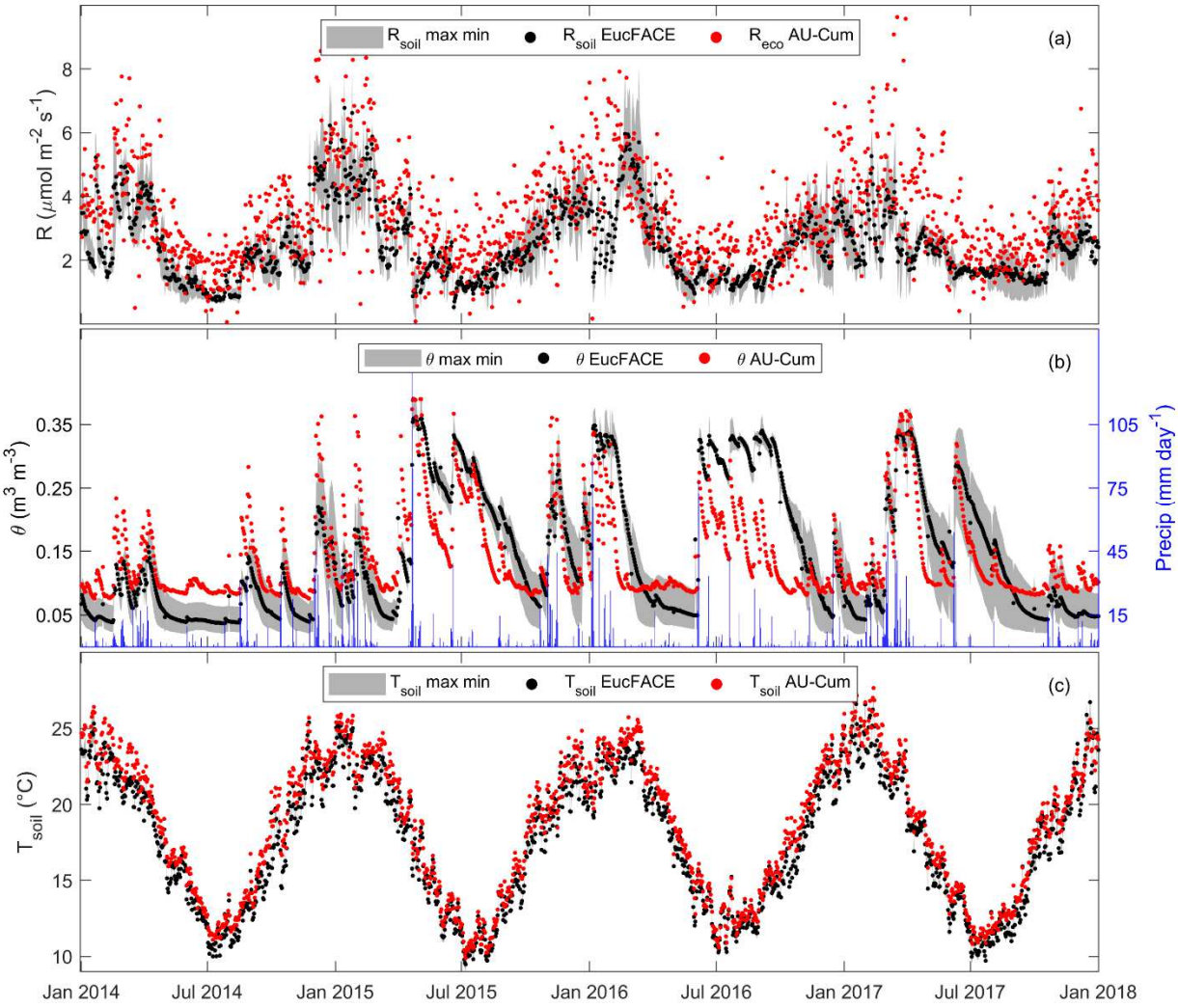

Figure 1 Time series of daily ecosystem respiration, soil respiration, soil moisture and soil temperature over the 2014-2017 period (n = 1462 days). (a) Night median respiration fluxes: black dots: EucFACE soil respiration (R_{soil}, gap-filled as in 2.4.2), red dots: AU-Cum flux tower ecosystem respiration (R_{eco}, gap-filled as in 2.3.3), (b) soil moisture (θ, m^3 m^{-3}) in shallow layer (5 cm for the flux site and 0-21 cm for EucFACE) and daily precipitation (mm day^{-1}) and (c) soil temperature (T_{soil}) at 5 cm depth. Black dots are the average of the three chambers or sensor, grey shade indicates the range of values across three chambers or sensors. Red dots are the median of night-time AU-Cum flux tower data.

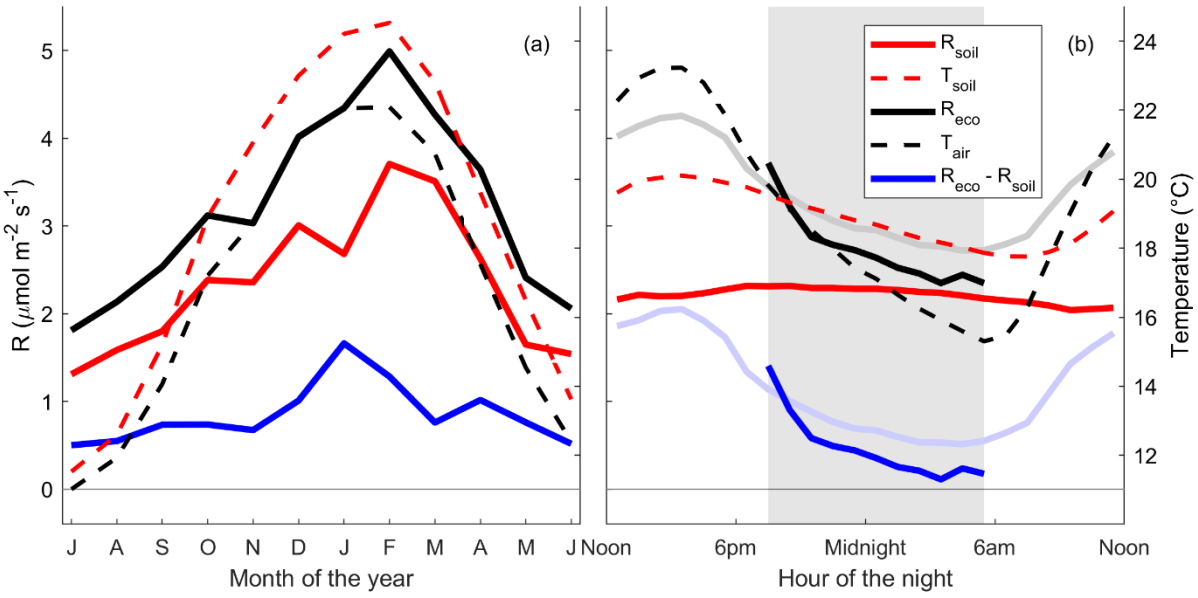

Figure 2 Seasonal and diurnal pattern of observed concurrent soil respiration, ecosystem respiration, above-ground respiration, soil temperature and air temperature. Temporal patterns of (a), monthly median of half-hourly night-time data (sunset to sunrise), and (b) diurnal pattern of hourly median of half-hourly data. Data shown: soil respiration (R_{soil}) and ecosystem respiration (R_{eco}), soil temperature (T_{soil}) and air temperature (T_{air}). $R_{eco} - R_{soil}$ is shown as an estimate of above-ground respiration. Data over the 4-year period 2014-2017 were used. In (a), only half-hourly observation of quality controlled R_{eco} (see 2.3.1) and concurrent R_{soil} were used. In (b), only observations (no gap-filling) of R_{soil} and R_{eco} are used to plot the bold colors (night-time), the grey line is gap-filled R_{eco} (as in 2.3.2), day and night, and the light blue line is gap-filled R_{eco} - R_{soil}. The grey shade represents night-time.

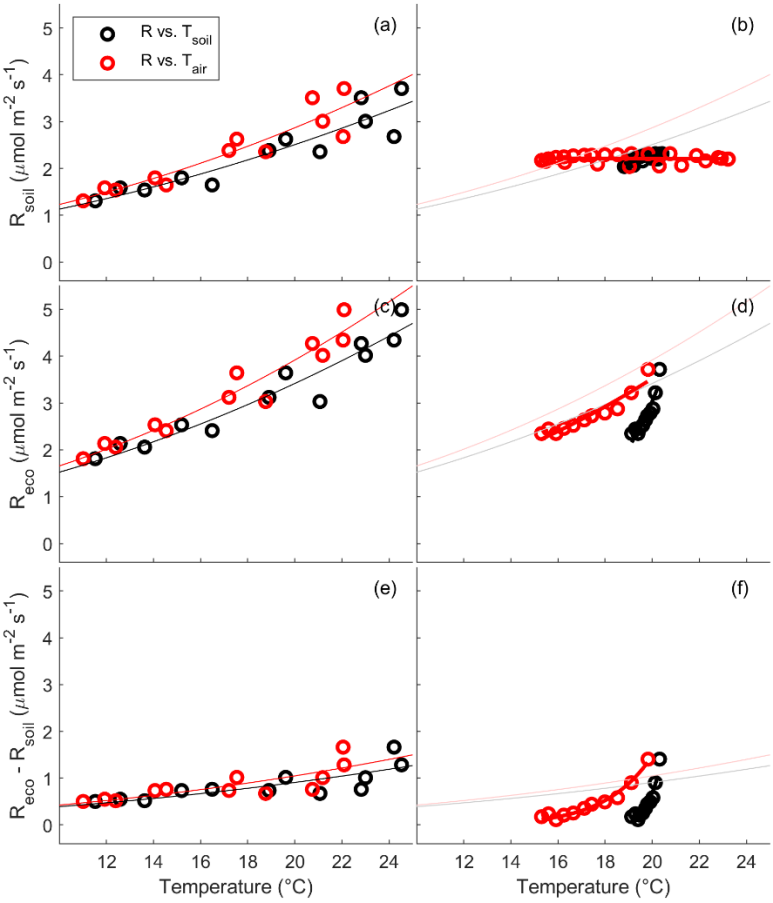

Figure 3 Apparent seasonal (monthly median, n = 12 months) and night-time (hourly median, n = 11 hours (R_{eco}) or n = 24 hours (R_{soil})) temperature responses (Lloyd & Taylor, 1994) of ecosystem respiration (R_{eco}), soil respiration (R_{soil}), and R_{eco} - R_{soil} (R_{AG} in theory). Night-time monthly (left panels) and hourly (right panels) medians were calculated as in Figure 2, only when both R_{soil} and R_{eco} observations were concurrently available. Monthly median of R_{soil} (a), R_{eco} (c) and R_{eco} - R_{soil} (e). Hourly median of R_{soil} (b), R_{eco} (d) and R_{eco} - R_{soil} (f). For comparison, lines from (a, c, e) and shown in panels (b, d, f) with lighter color. Parameter values and quality of fit are reported in Table 1.

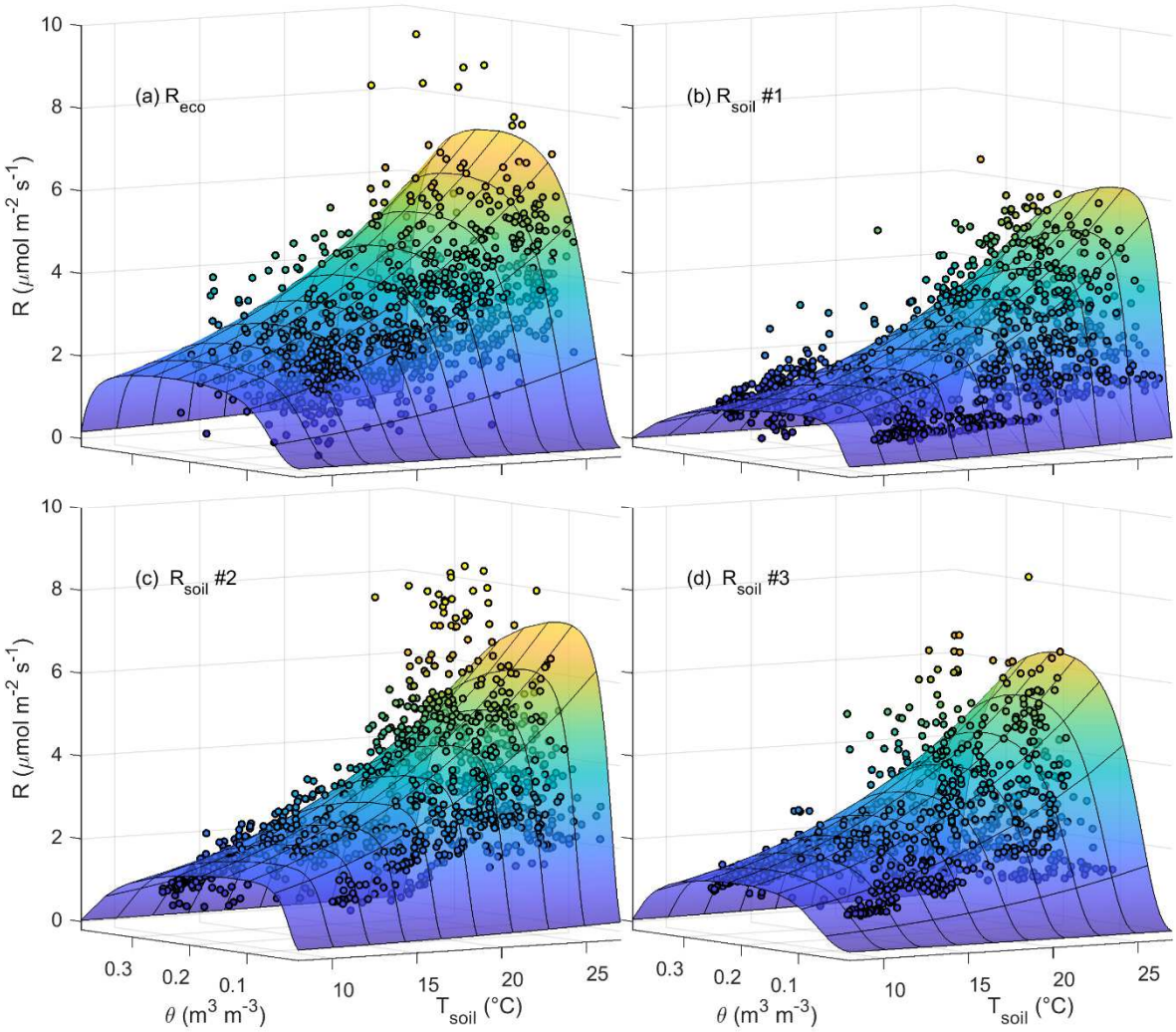

Figure 4 Daily (night median) response of ecosystem respiration (a) and soil respiration at three individual collar locations (b-d) to soil temperature and soil moisture (dots), and Dual-Arrhenius Michaelis Menten (DAMM) model fit (surface). Values of fitted parameters and quality of fit are reported in Table 2. Only measurements are used in to fit the model (no gap-filled data).

Table 1 Parameter values (E_0 and R_{10} and quality of fit, r^2) of the Lloyd and Taylor model fitted to monthly (seasonal) or hourly (diurnal) ecosystem respiration (R_{eco}), soil respiration (R_{soil}) and above-ground respiration ($R_{eco} - R_{soil}$). The monthly median and hourly median of R_{soil}, R_{eco} and R_{eco} - R_{soil} vs. T_{soil} and T_{air}. Observations (not gapfilled estimates) over 2014-2017 were used to calculate medians.

Component	Temperature	**Month medians (n = 12)**			**Hour average (R_{soil} n = 24; R_{eco} n = 11)**		
		E_0	**R_{10}**	**R^2**	**E_0**	**R_{10}**	**R^2**
R_{soil}	T_{soil}	301	1.19	0.80	235	1.28	0.93
	T_{air}	319	1.29	0.80	29	2.22	0.36
R_{eco}	T_{soil}	299	1.52	0.93	1626	0.04	0.86
	T_{air}	319	1.65	0.93	402	1.21	0.91
R_{eco} - R_{soil}	T_{soil}	294	0.33	0.47	7459	0.00	0.84
	T_{air}	318	0.36	0.48	2836	0.00	0.98

Table 2 Fitted parameters values and quality of fit of the semi-mechanistic Dual Arrhenius and Michaelis Menten (DAMM) model (Figure 4) fitted to night-time observations of R_{soil} of three individual collar locations and R_{eco}, using half-hourly night data or the median of nighttime data comprised of all nights with at least 10 half-hours of available data, over the 4-year period 2014-2017.

Data time resolution	**Fit to**	**Fitted parameters**				**r^2**	**RMSE**	**n**
		α_{Sx}	**Ea**	**kM_{SX}**	**kM_{O2}**			
Half-hourly	R_{soil} 1	8.5E+06	54	2.6E-08	1.2E-02	0.62	0.80	52079
	R_{soil} 2	1.3E+06	49	3.2E-08	6.9E-03	0.66	0.89	44283
	R_{soil} 3	1.1E+06	49	5.0E-07	4.0E-03	0.53	0.89	37461
	$R_{soil, mean}$	3.6E+06	51	1.9E-07	7.5E-03	0.60	0.86	44608
	R_{eco}	**5.1E+04**	**42**	**2.5E-07**	**1.2E-03**	**0.10**	**2.43**	**15686**
Nightly	R_{soil} 1	2.2E+08	62	2.3E-08	1.1E-02	0.69	0.71	1116
	R_{soil} 2	2.7E+07	57	3.1E-08	9.2E-03	0.72	0.85	1037
	R_{soil} 3	6.9E+07	59	5.0E-07	4.4E-03	0.59	0.83	869
	$R_{soil, mean}$	1.0E+08	59	1.9E-07	8.1E-03	0.66	0.79	1007
	R_{eco}	**4.5E+06**	**52**	**3.6E-07**	**1.5E-03**	**0.50**	**1.05**	**933**

Table 3 Quality of fit (R^2 and RMSE) of models fitted on night-time observation of ecosystem respiration (R_{eco}), using half-hourly night data (top) or the median of night data with at least 10 half-hours (bottom), for different environment driver sets. R^2 Δ and RMSE Δ shows the improvement of models when using the same drivers and including soil respiration (R_{soil}) as an additional driver.

	Model	Drivers	R^2	R^2 Δ	RMSE	RMSE Δ
half-hourly (n = 15686)	LT	T_{air}	0.08		2.45	
	LT	T_{soil}	0.08		2.46	
	DAMM	**T_{soil}, θ**	**0.10**		**2.43**	
	ANN	T_{air}	0.09		2.45	
	ANN	T_{soil}	0.09		2.45	
	ANN	**T_{soil}, θ**	**0.10**		**2.43**	
	ANN	T_{soil}, T_{air}, θ	0.11		2.41	
	ANN	R_{soil}	0.09		2.45	
	ANN	R_{soil}, T_{air}	0.11	0.02	2.42	-0.03
	ANN	R_{soil}, T_{soil}	0.10	0.01	2.43	-0.02
	ANN	R_{soil}, T_{soil}, θ	0.11	0.00	2.42	-0.01
	ANN	R_{soil}, T_{soil}, T_{air}, θ	0.12	0.00	2.41	-0.01
	ANN	3 R_{soil},3 θ, T_{soil}, T_{air}	0.12		2.40	
Average night-time (n = 933)	LT	T_{air}	0.36		1.18	
	LT	T_{soil}	0.39		1.16	
	DAMM	**T_{soil}, θ**	**0.50**		**1.05**	
	ANN	T_{air}	0.37		1.18	
	ANN	T_{soil}	0.41		1.13	
	ANN	**T_{soil}, θ**	**0.53**		**1.01**	
	ANN	T_{soil}, T_{air}, θ	0.55		0.99	
	ANN	R_{soil}	0.44		1.11	
	ANN	R_{soil}, T_{air}	0.50	0.13	1.05	-0.12
	ANN	R_{soil}, T_{soil}	0.49	0.08	1.06	-0.08
	ANN	R_{soil}, T_{soil}, θ	0.55	0.02	1.00	-0.02
	ANN	R_{soil}, T_{soil}, T_{air}, θ	0.57	0.01	0.98	-0.02
	ANN	3 R_{soil}, 3 θ, T_{soil}, T_{air}	0.58		0.96	

References

Aspinwall, M. J., Drake, J. E., Campany, C., Vårhammar, A., Ghannoum, O., Tissue, D. T., . . . Tjoelker, M. G. (2016). Convergent acclimation of leaf photosynthesis and respiration to prevailing ambient temperatures under current and warmer climates in Eucalyptus tereticornis. *New Phytologist, 212*(2), 354-367.

Atkin, O., Holly, C., & Ball, M. (2000). Acclimation of snow gum (Eucalyptus pauciflora) leaf respiration to seasonal and diurnal variations in temperature: the importance of changes in the capacity and temperature sensitivity of respiration. *Plant, Cell & Environment, 23*(1), 15-26.

Aubinet, M., Berbigier, P., Bernhofer, C., Cescatti, A., Feigenwinter, C., Granier, A., . . . Longdoz, B. (2005). Comparing CO 2 storage and advection conditions at night at different carboeuroflux sites. *Boundary-Layer Meteorology, 116*(1), 63-93.

Aubinet, M., Feigenwinter, C., Heinesch, B., Bernhofer, C., Canepa, E., Lindroth, A., . . . Van Gorsel, E. (2010). Direct advection measurements do not help to solve the night-time CO2 closure problem: Evidence from three different forests. *Agricultural and Forest Meteorology, 150*(5), 655-664.

Aubinet, M., Grelle, A., Ibrom, A., Rannik, Ü., Moncrieff, J., Foken, T., . . . Bernhofer, C. (1999). Estimates of the annual net carbon and water exchange of forests: the EUROFLUX methodology. In *Advances in ecological research* (Vol. 30, pp. 113-175): Elsevier.

Aubinet, M., Grelle, A., Ibrom, A., Rannik, U., Moncrieff, J., Foken, T., . . . Vesala, T. (2000). Estimates of the annual net carbon and water exchange of forests: The EUROFLUX methodology. *Advances in Ecological Research, Vol 30, 30*, 113-175.

Aubinet, M., Vesala, T., & Papale, D. (2012). *Eddy Covariance A Practical Guide to Measurement and Data Analysis*: Springer.

Baldocchi, D. D., Hicks, B. B., & Meyers, T. P. (1988). MEASURING BIOSPHERE-ATMOSPHERE EXCHANGES OF BIOLOGICALLY RELATED GASES WITH MICROMETEOROLOGICAL METHODS. *Ecology, 69*(5), 1331-1340. doi:10.2307/1941631

Barba, J., Cueva, A., Bahn, M., Barron-Gafford, G. A., Bond-Lamberty, B., Hanson, P. J., . . . Scott, R. L. (2018). Comparing ecosystem and soil respiration: Review and key challenges of tower-based and soil measurements. *Agricultural and Forest Meteorology, 249*, 434-443.

Barr, A., Richardson, A., Hollinger, D., Papale, D., Arain, M., Black, T., . . . Gu, L. (2013). Use of change-point detection for friction–velocity threshold evaluation in eddy-covariance studies. *Agricultural and Forest Meteorology, 171*, 31-45.

Belcher, S. E., Harman, I. N., & Finnigan, J. J. (2012). The wind in the willows: flows in forest canopies in complex terrain. *Annual Review of Fluid Mechanics, 44*, 479-504.

Bond□Lamberty, B., Christianson, D. S., Malhotra, A., Pennington, S. C., Sihi, D., AghaKouchak, A., . . . Ashraf, S. (2020). COSORE: A community database for continuous soil respiration and other soil□atmosphere greenhouse gas flux data. *Global change biology, 26*(12), 7268-7283.

Crous, K. Y., ZARAGOZA□CASTELLS, J., Ellsworth, D. S., Duursma, R. A., Loew, M., Tissue, D. T., & Atkin, O. K. (2012). Light inhibition of leaf respiration in field□grown Eucalyptus saligna in whole□tree chambers under elevated atmospheric CO2 and summer drought. *Plant, Cell & Environment, 35*(5), 966-981.

Crous, K. Y., ZARAGOZA□CASTELLS, J., Loew, M., Ellsworth, D. S., Tissue, D. T., Tjoelker, M. G., . . . Atkin, O. K. (2011). Seasonal acclimation of leaf respiration in Eucalyptus saligna trees: impacts of elevated atmospheric CO2 and summer drought. *Global Change Biology, 17*(4), 1560-1576.

Cueva, A., Bahn, M., Litvak, M., Pumpanen, J., & Vargas, R. (2015). A multisite analysis of temporal random errors in soil CO2 efflux. *Journal of Geophysical Research: Biogeosciences, 120*(4), 737-751.

Davidson, E. A., Samanta, S., Caramori, S. S., & Savage, K. (2012). The D ual A rrhenius and M ichaelis–M enten kinetics model for decomposition of soil organic matter at hourly to seasonal time scales. *Global change biology, 18*(1), 371-384.

Desai, A. R., Richardson, A. D., Moffat, A. M., Kattge, J., Hollinger, D. Y., Barr, A., . . . Stauch, V. J. (2008). Cross-site evaluation of eddy covariance GPP and RE decomposition techniques. *Agricultural and Forest Meteorology, 148*(6-7), 821-838. doi:10.1016/j.agrformet.2007.11.012

Drake, J. E., Furze, M. E., Tjoelker, M. G., Carrillo, Y., Barton, C. V., & Pendall, E. (2019). Climate warming and tree carbon use efficiency in a whole□tree 13 CO 2 tracer study. *New Phytologist, 222*(3), 1313-1324.

Drake, J. E., Macdonald, C. A., Tjoelker, M. G., Reich, P. B., Singh, B. K., Anderson, I. C., & Ellsworth, D. S. (2018). Three years of soil respiration in a mature eucalypt woodland exposed to atmospheric CO 2 enrichment. *Biogeochemistry, 139*(1), 85-101.

Drake, J. E., Tjoelker, M. G., Aspinwall, M. J., Reich, P. B., Barton, C. V., Medlyn, B. E., & Duursma, R. A. (2016). Does physiological acclimation to climate warming stabilize the ratio of canopy respiration to photosynthesis? *New Phytologist, 211*(3), 850-863.

Foken, T., Gockede, M., Mauder, M., Mahrt, L., Amiro, B., & Munger, W. (2004). Post-field data quality control. *Handbook of Micrometeorology: A Guide for Surface Flux Measurement and Analysis, 29*, 181-208.

Friedlingstein, P., Jones, M., O'Sullivan, M., Andrew, R., Hauck, J., Peters, G., . . . Le Quéré, C. (2019). Global carbon budget 2019. *Earth System Science Data, 11*(4), 1783-1838.

Giasson, M.-A., Ellison, A. M., Bowden, R. D., Crill, P. M., Davidson, E. A., Drake, J. E., . . . Melillo, J. M. (2013). Soil respiration in a northeastern US temperate forest: a 22□year synthesis. *Ecosphere, 4*(11), 1-28.

Griebel, A., Metzen, D., Boer, M. M., Barton, C. V., Renchon, A. A., Andrews, H. M., & Pendall, E. (2020). Using a paired tower approach and remote sensing to assess carbon sequestration and energy distribution in a heterogeneous sclerophyll forest. *Science of the Total Environment, 699*, 133918.

Hayek, M. N., Wehr, R., Longo, M., Hutyra, L. R., Wiedemann, K., Munger, J. W., . . . Wofsy, S. C. (2018). A novel correction for biases in forest eddy covariance carbon balance. *Agricultural and Forest Meteorology, 250*, 90-101.

Heinemeyer, A., Hartley, I. P., Evans, S. P., Carreira de La Fuente, J. A., & Ineson, P. (2007). Forest soil CO2 flux: uncovering the contribution and environmental responses of ectomycorrhizas. *Global Change Biology, 13*(8), 1786-1797.

Heskel, M. A., Atkin, O. K., Turnbull, M. H., & Griffin, K. L. (2013). Bringing the Kok effect to light: a review on the integration of daytime respiration and net ecosystem exchange. *Ecosphere, 4*(8), 1-14.

Hollinger, D., & Richardson, A. (2005). Uncertainty in eddy covariance measurements and its application to physiological models. *Tree Physiology, 25*(7), 873-885.

Keenan, T., Migliavacca, M., Papale, D., Baldocchi, D., Reichstein, M., Torn, M., & Wutzler, T. (2018). *Inhibition of leaf respiration by light: implications for eddy-covariance partitioning.* Paper presented at the EGU General Assembly Conference Abstracts.

Keenan, T. F., Migliavacca, M., Papale, D., Baldocchi, D., Reichstein, M., Torn, M., & Wutzler, T. (2019). Widespread inhibition of daytime ecosystem respiration. *Nature ecology & evolution, 3*(3), 407-415.

King, A. W., Gunderson, C. A., Post, W. M., Weston, D. J., & Wullschleger, S. D. (2006). Plant respiration in a warmer world. *Science, 312*(5773), 536-537.

Kok, B. (1949). On the interrelation of respiration and photosynthesis in green plants. *Biochimica et biophysica acta, 3*, 625-631.

Lasslop, G., Reichstein, M., Papale, D., Richardson, A. D., Arneth, A., Barr, A., . . . Wohlfahrt, G. (2010). Separation of net ecosystem exchange into assimilation and respiration using a light response curve approach: critical issues and global evaluation. *Global Change Biology, 16*(1), 187-208.

Law, B. E., Ryan, M. G., & Anthoni, P. M. (1999). Seasonal and annual respiration of a ponderosa pine ecosystem. *Global Change Biology, 5*(2), 169-182.

Leuning, R., Zegelin, S. J., Jones, K., Keith, H., & Hughes, D. (2008). Measurement of horizontal and vertical advection of CO2 within a forest canopy. *Agricultural and Forest Meteorology, 148*(11), 1777-1797.

Lloyd, J., & Taylor, J. A. (1994). ON THE TEMPERATURE-DEPENDENCE OF SOIL RESPIRATION. *Functional Ecology, 8*(3), 315-323. doi:10.2307/2389824

McHugh, I. D., Beringer, J., Cunningham, S. C., Baker, P. J., Cavagnaro, T. R., Mac Nally, R., & Thompson, R. M. (2017). Interactions between nocturnal turbulent flux, storage and advection at an "ideal" eucalypt woodland site. *Biogeosciences, 14*(12), 3027-3050.

Mitra, B., Mackay, D.S., Pendall, E., Ewers, B.E., & Cleary, M.B. (2014). Does vegetation structure regulate the spatial structure of soil respiration within a sagebrush steppe ecosystem? *Journal of Arid Environments* 103: 1-10.

Moffat, A. M., Papale, D., Reichstein, M., Hollinger, D. Y., Richardson, A. D., Barr, A. G., . . . Desai, A. R. (2007). Comprehensive comparison of gap-filling techniques for eddy covariance net carbon fluxes. *Agricultural and Forest Meteorology, 147*(3-4), 209-232.

Ohkubo, S., Kosugi, Y., Takanashi, S., Mitani, T., & Tani, M. (2007). Comparison of the eddy covariance and automated closed chamber methods for evaluating nocturnal CO2 exchange in a Japanese cypress forest. *Agricultural and Forest Meteorology, 142*(1), 50-65.

Phillips, C. L., Bond-Lamberty, B., Desai, A. R., Lavoie, M., Risk, D., Tang, J., . . . Vargas, R. (2017). The value of soil respiration measurements for interpreting and modeling terrestrial carbon cycling. *Plant and Soil, 413*(1-2), 1-25.

Pumpanen, J., Kolari, P., Ilvesniemi, H., Minkkinen, K., Vesala, T., Niinistö, S., . . . Pihlatie, M. (2004). Comparison of different chamber techniques for measuring soil CO2 efflux. *Agricultural and Forest Meteorology, 123*(3-4), 159-176.

Reichstein, M., Falge, E., Baldocchi, D., Papale, D., Aubinet, M., Berbigier, P., . . . Valentini, R. (2005). On the separation of net ecosystem exchange into assimilation and ecosystem respiration: review and improved algorithm. *Global Change Biology, 11*(9), 1424-1439. doi:10.1111/j.1365-2486.2005.001002.x

Renchon, A. A., Griebel, A., Metzen, D., Williams, C. A., Medlyn, B., Duursma, R. A., . . . Isaac, P. (2018). Upside-down fluxes Down Under: CO 2 net sink in winter and net source in summer in a temperate evergreen broadleaf forest. *Biogeosciences, 15*(12), 3703-3716.

Richardson, A. D., Braswell, B. H., Hollinger, D. Y., Burman, P., Davidson, E. A., Evans, R. S., . . . Urbanski, S. P. (2006). Comparing simple respiration models for eddy flux and dynamic chamber data. *Agricultural and Forest Meteorology, 141*(2-4), 219-234.

Savage, K.E., and Davidson, E.A. (2003). A comparison of manual and automated systems for soil CO_2 flux measurements: tradeoffs between spatial and temporal resolution. *Journal of Experimental Botany* 54:891-899.

Sihi, D., Davidson, E. A., Chen, M., Savage, K. E., Richardson, A. D., Keenan, T. F., & Hollinger, D. Y. (2018). Merging a mechanistic enzymatic model of soil heterotrophic respiration into an ecosystem model in two AmeriFlux sites of northeastern USA. *Agricultural and Forest Meteorology, 252*, 155-166.

Speckman, H. N., Frank, J. M., Bradford, J. B., Miles, B. L., Massman, W. J., Parton, W. J., & Ryan, M. G. (2015). Forest ecosystem respiration estimated from eddy covariance and chamber measurements under high turbulence and substantial tree mortality from bark beetles. *Global Change Biology, 21*(2), 708-721.

Thomas, C. K., Martin, J. G., Law, B. E., & Davis, K. (2013). Toward biologically meaningful net carbon exchange estimates for tall, dense canopies: multi-level eddy covariance observations and canopy coupling regimes in a mature Douglas-fir forest in Oregon. *Agricultural and Forest Meteorology, 173*, 14-27.

Tozer, M. (2003). The native vegetation of the Cumberland Plain, western Sydney: systematic classification and field identification of communities. *Cunninghamia, 8*(1), 1-75.

Van Gorsel, E., Harman, I. N., Finnigan, J. J., & Leuning, R. (2011). Decoupling of air flow above and in plant canopies and gravity waves affect micrometeorological estimates of net scalar exchange. *Agricultural and Forest Meteorology, 151*(7), 927-933.

Van Gorsel, E., Leuning, R., Cleugh, H. A., Keith, H., & Suni, T. (2007). Nocturnal carbon efflux: reconciliation of eddy covariance and chamber measurements using an alternative to the u.-threshold filtering technique. *Tellus B: Chemical and Physical Meteorology, 59*(3), 397-403.

Vargas, R., Carbone, M. S., Reichstein, M., & Baldocchi, D. D. (2011). Frontiers and challenges in soil respiration research: from measurements to model-data integration. *Biogeochemistry, 102*(1-3), 1-13.

Wang, X., Wang, C., & Bond-Lamberty, B. (2017). Quantifying and reducing the differences in forest CO2-fluxes estimated by eddy covariance, biometric and chamber methods: A global synthesis. *Agricultural and Forest Meteorology, 247*, 93-103.

Way, D. A., Aspinwall, M. J., Drake, J. E., Crous, K. Y., Campany, C. E., Ghannoum, O., . . . Tjoelker, M. G. (2019). Responses of respiration in the light to warming in field□grown trees: a comparison of the thermal sensitivity of the Kok and Laisk methods. *New Phytologist, 222*(1), 132-143.

Wehr, R., Munger, J., McManus, J., Nelson, D., Zahniser, M., Davidson, E., . . . Saleska, S. (2016). Seasonality of temperate forest photosynthesis and daytime respiration. *Nature, 534*(7609), 680.

Supporting References

Gimeno, T. E., McVicar, T. R., O'Grady, A. P., Tissue, D. T., & Ellsworth, D. S. (2018). Elevated CO2 did not affect the hydrological balance of a mature native Eucalyptus woodland. *Global Change Biology*, 24(7), 3010-3024.

Griebel, A., Metzen, D., Boer, M. M., Barton, C. V. M., Renchon, A. A., Andrews, H., & Pendall, E. (2020). Using a paired tower approach and remote sensing to assess carbon sequestration and energy distribution in a heterogeneous sclerophyll forest. *Science of the Total Environment*, 699, 133918.

Jiang, M. K., Medlyn, B. E., Drake, J. E., Duursma, R. A., Anderson, I. C., Barton, C. V. M., et al. (2020). The fate of carbon in a mature forest under carbon dioxide enrichment. *Nature*, 580(7802), 227-+.

Karan, M., Liddell, M., Prober, S. M., Arndt, S., Beringer, J., Boer, M., et al. (2016). The Australian SuperSite Network: A continental, long-term terrestrial ecosystem observatory. *Science of the Total Environment*, 568, 1263-1274.

Liu, L., Lim, S. S., Shen, X. S., & Yebra, M. (2020). Assessment of generalized allometric models for aboveground biomass estimation: A case study in Australia. *Computers and Electronics in Agriculture*, 175.

Renchon, A. A., Griebel, A., Metzen, D., Williams, C. A., Medlyn, B. E., Duursma, R. A., et al. (2018). Upside-down fluxes Down Under: CO2 net sink in winter and net source in summer in a temperate evergreen broadleaf forest. *Biogeosciences,* 15, 3703-3716.